Acta Crystallographica Section B
Structural Science
ISSN 0108-7681

Inverse bilayer structure of mononuclear Co^{II} and Ni^{II} complexes of the type $M(H_2O)_3(SO_4)(4\text{-CNpy})_2$

Birinchi K. Das,* Sanchay J. Bora, Manjit K. Bhattacharyya and Rama K. Barman‡

Department of Chemistry, Gauhati University, Guwahati 781 014, Assam, India

‡ Present address: Department of Chemistry, Sherubtse College, Royal University of Bhutan, Kanglung, Trashigang, Bhutan.

Correspondence e-mail:
birinchi.das@hotmail.com

Received 24 December 2008
Accepted 3 June 2009

Two new metal compounds of the formula $[M(H_2O)_3(SO_4)(4\text{-CNpy})_2]\cdot H_2O$ [M = Ni (1) and Co (2), 4-CNpy = 4-cyanopyridine] have been prepared and studied by X-ray diffraction. In both of these compounds the 4-CNpy ligands are coordinated *via* pyridyl-N atoms to the metal ions in a *cis* fashion. The neutral complexes along with the uncoordinated H_2O molecules are glued together preferentially into inverse bilayers by non-covalent interactions, including unique inter-layer π–π interactions between antiparallel nitrile groups. Hartree–Fock and density-functional theory (DFT) calculations indicate that the π–π interactions are energetically significant. The unit-cell similarity index (Π) of 0.0046 for the compounds suggests their isostructurality, which is also supported by their X-ray powder diffraction patterns that can be almost superimposed.

1. Introduction

Intermolecular interactions often govern molecular arrangements in crystals (Desiraju, 2001). In view of the importance of non-covalent forces in determining supramolecular structures, ligand systems containing both electron donor and acceptor sites may be expected to lead to interesting assemblies of metal-organic compounds. As an example, 4-cyanopyridine (I) containing an electron-withdrawing nitrile group as the acceptor and the pyridyl nitrogen as the donor represents a suitable ligand for this purpose (Barman & Das, 2002). The presence of two regions of delocalized electron density also brings in the possibility of π–π interactions so as to direct preferences for thermodynamically favoured solid-state structures.

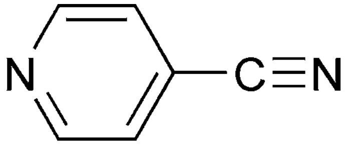
(I)

With a view to demonstrating the structure-directing influence of (I) we herein describe two analogous Co^{II} and Ni^{II} complexes of the type $M(H_2O)_3(SO_4)(4\text{-CNpy})_2\cdot H_2O$, with M = Ni (1), Co (2), which contain the 4-substituted pyridine (I) as a ligand. It may be mentioned here that (1) has been recently described as a synthetic precursor to obtain other crystalline supramolecular coordination solids (Bhattacharyya *et al.*, 2008). Also, these species are useful as starting materials for preparing coordination polymers (Bora & Das, 2009).

It will be seen that both compounds discussed here have a novel two-dimensional structure, closely akin to clay mimics (Holman *et al.*, 2001; Beatty *et al.*, 2002; Biradha *et al.*, 1998). It is also noted that the crystal structures described herein

doi:10.1107/S0108768109021090

resemble the 'inverse bilayer' structure identified previously (Raghavaiah *et al.*, 2005; Janiak, 2006). What is unique about the present results is that unlike in earlier cases where salts of organic cations have been shown to organize into bilayers consisting of hydrophilic interior regions and hydrophobic exterior regions, the bilayer formation in (1) and (2) involves monohydrated metal complexes which are charge-neutral. In this paper we shall discuss the various non-covalent interactions involved in the formation of the lamellar structures of (1) and (2). In addition, the evaluation of the isostructurality of (1) and (2) will also be described in this paper.

2. Experimental

2.1. Materials and methods

Reagents and solvents used in this work were obtained from commercial sources and used as received. While the metal sulfate hydrates were purchased from E. Merck (India), 4-cyanopyridine was procured from Aldrich (USA). The C–H–N analyses were performed using a Perkin-Elmer 2400 Series II CHNS/O Analyzer. FT-IR spectra were recorded using a Perkin-Elmer RX1 spectrophotometer in the mid-IR region (4000 to 450 cm^{-1}) for KBr pellets. The computation of stabilization energies resulting from π–π forces was carried out using *GAUSSIAN*03W (Frisch *et al.*, 2004) using 6-31G(d) basis sets. Atomic coordinates were extracted from the crystallographically determined structure of (1) (see below) to prepare the necessary *GAUSSIAN*03 input file. The DFT calculation was performed using the B3LYP functional. The evaluation of isostructurality was carried out using a previously developed method (Fábián & Kálmán, 1999).

2.2. Synthesis of compounds

2.2.1. $Ni(H_2O)_3(SO_4)(4\text{-CNpy})_2\cdot H_2O$ (1). A mixture of $NiSO_4\cdot 7H_2O$ (1.120 g, 4 mmol) and 4-cyanopyridine (0.832 g, 8 mmol), dissolved in 1:1 water/methanol (20 ml), was mechanically stirred at room temperature for 12 h. The blue precipitate formed was filtered, washed with small volumes of water under suction and then with methanol, and dried in a vacuum desiccator over fused $CaCl_2$. Yield: 1.14 g, 66%. Anal.: calc. for $C_{12}H_{16}N_4O_8SNi$: C 33.12, H 3.67, N 12.88; found: C 33.59, H 3.32, N 12.32. IR spectral data (KBr disc, cm^{-1}): 3277(br), 2926(w), 2238(w), 1668(w), 1608(s), 1548(m), 1493(m), 1414(m), 1219(w), 1106(s, br), 1026(sh), 986(sh), 840(s), 778(w), 618(m), 566(w) [s, strong; m, medium; w, weak; br, broad].

2.2.2. $Co(H_2O)_3(SO_4)(4\text{-CNpy})_2\cdot H_2O$ (2). A mixture of $CoSO_4\cdot 7H_2O$ (1.124 g, 4 mmol) and 4-cyanopyridine (0.832 g, 8 mmol), dissolved in 1:1 water/methanol (20 ml), was mechanically stirred at room temperature for 6 h. The pink precipitate formed was filtered, washed with small volumes of water under suction and then with methanol, and dried in a vacuum desiccator over fused $CaCl_2$. Yield: 1.07 g (62%). Anal.: calc. for $C_{12}H_{16}N_4O_8SCo$: C 33.11, H 3.68, N 12.88 (%); found: C 33.41, H 3.72, N 13.23 (%). IR spectral data (KBr disc, cm^{-1}): 3436(s, br), 3351(s, br), 2241(w), 1658(sh), 1606(s), 1545(m), 1498(m), 1458(w), 1414(s), 1215(w), 1114(s, br), 1016(sh), 984(sh), 834(s), 778(w), 620(m), 562(m) [s, strong; m, medium; w, weak; br, broad].

To obtain crystals of the desired quality for single-crystal X-ray diffraction work, mixtures of 1 mmol of MSO$_4\cdot$7H$_2$O and 2 mmol of 4-CNpy were refluxed for 30 min in 10 ml of 1:1 MeOH/H_2O and the resulting solutions gave suitable crystals for X-ray studies upon cooling.

2.3. X-ray crystallographic procedures

For intensity data collection crystals of suitable size were mounted on glass fibres at room temperature using graphite-monochromated Mo $K\alpha$ radiation on a Bruker SMART CCD diffractometer (Bruker AXS Inc., 2004*a*,*b*). The data were processed as described earlier (Chakrabarty *et al.*, 2007). The crystals were found to be stable against intensity decay. The structures were solved by the direct method (*SHELXS*) and refined by full-matrix least-squares techniques (*SHELXL*) with *SHELX*97 (Sheldrick, 2008) using the *WinGX* (Farrugia, 1999) platform available for personal computers. The H atoms of the water molecules in both compounds were located in difference-Fourier maps and refined with isotropic atomic displacement parameters, while the aromatic ring H atoms were placed at calculated positions. All other atoms were refined with anisotropic displacement parameters. The crystal structures were analysed with *PLUTON* (Spek, 1990) and *Mercury*1.4.2 (Macrae *et al.*, 2006), while the structural diagrams were drawn using *DIAMOND* (Brandenburg, 2008).

X-ray powder diffraction patterns in the 3–60° 2θ range were recorded using a Philips X'Pert PRO instrument using Cu $K\alpha$ radiation (1.5418 Å) with a scan rate of 0.5 s (0.5° 2θ) per step at 40 kV/30 mA. The calculated diffraction patterns, assuming Bragg–Brentano geometry, were obtained from results of single-crystal structure analyses using the computer program *PowderCell* (Kraus & Nolze, 2000). The X-ray powder diffraction patterns were drawn using *Origin*8.0 (OriginLab, 2007). Peak indexing was carried out by comparing the 2θ values and relative intensities of the experimental and calculated patterns.

3. Results and discussion

3.1. Preparation and physicochemical properties

The compounds $[M(4\text{-CNpy})_2(H_2O)_3(SO_4)]\cdot H_2O$, M = Ni (1), Co (2), have been prepared in good yield by a straightforward self-assembly process involving MSO$_4\cdot$7H$_2$O and 4-CNpy in an H_2O/MeOH mixture (1:1, v/v) at room temperature. Physically, both compounds are inhomogeneous powders interspersed with small crystals of varying dimension and shape. The blue-coloured nickel(II) compound (1) dissolves slowly in water, but it does not dissolve in common organic solvents. The solubility of the lightly pink cobalt(II) compound (2) in water is somewhat more pronounced, but it is also insoluble in organic solvents like (1).

In the IR spectrum, bands due to the pyridine ring vibrations of 4-cyanopyridine in (1) are observed at 1608, 1548,

Table 1
Experimental details.

	(1)	(2)
Crystal data		
Chemical formula	$C_{12}H_{16}N_4NiO_8S$	$C_{12}H_{16}CoN_4O_8S$
M_r	435.06	435.28
Crystal system, space group	Monoclinic, $P2_1/c$	Monoclinic, $P2_1/c$
Temperature (K)	293	293
a, b, c (Å)	17.2117 (8), 8.4275 (4), 12.5984 (6)	17.1467 (3), 8.3504 (1), 12.5644 (2)
β (°)	94.644 (1)	94.509 (1)
V (Å^3)	1821.4 (2)	1793.43 (5)
Z	4	4
Radiation type	Mo $K\alpha$	Mo $K\alpha$
μ (mm^{-1})	1.23	1.12
Crystal form, size (mm)	Rectangular block, 0.40 × 0.35 × 0.20	Rectangular block, 0.42 × 0.37 × 0.11
Data collection		
Diffractometer	Bruker AXS CCD	Bruker AXS CCD
Data collection method	φ and ω scans	φ and ω scans
Absorption correction	Multi-scan†	Multi-scan†
$T_{\min}$	0.757	0.854
$T_{\max}$	1.000	1.000
No. of measured, independent and observed reflections	10 611, 4058, 3447	19 138, 4431, 3899
Criterion for observed reflections	$I > 2\sigma(I)$	$I > 2\sigma(I)$
$R_{\rm int}$	0.018	0.024
$\theta_{\max}$ (°)	28.0	28.3
Refinement		
Refinement on	F^2	F^2
$R[F^2 > 2\sigma(F^2)]$, $wR(F^2)$, S	0.025, 0.064, 1.03	0.026, 0.072, 1.03
No. of reflections	4058	4431
No. of parameters	268	267
H-atom treatment	Mixture‡	Mixture‡
$(\Delta/\sigma)_{\max}$	0.001	0.001
$\Delta\rho_{\max}$, $\Delta\rho_{\min}$ (e Å^{-3})	0.30, −0.33	0.53, −0.30
Extinction method	*SHELXL*	None
Extinction coefficient	0.0026 (4)	–

Computer programs used: *SHELXS*97 (Sheldrick, 2008), *SHELXL*97 (Sheldrick, 2008). † Based on symmetry-related measurements. ‡ Mixture of independent and constrained refinement.

1493 and 840 cm^{-1}. The corresponding bands for (2) are found to occur at 1606, 1545, 1498 and 834 cm^{-1}. The C≡N vibration bands for (1) and (2) are observed at 2238 and 2241 cm^{-1}. Since these values are very close to 2243 cm^{-1}, where the ν(C≡N) vibration of free 4-CNpy occurs, it may be surmised that metal coordination of 4-CNpy has little influence on the triple-bond vibration in (1) and (2). Clearly the metal coordination has not occurred *via* the nitrile-N of 4-CNpy. The presence of the sulfate ion in the compounds is indicated by strong and broad absorption envelopes centering at ~ 1110 cm^{-1} in these compounds. This band perhaps occurs (Cotton & Wilkinson, 1988; Nakamoto, 1978) due to a merger of the ν_{3a} and ν_{3b} bands for unidentate SO_4^{2-}, which are expected to occur in the spectral ranges 1032–1044 and 1117–1143 cm^{-1}. The ν(OH) stretching vibrations are seen as broad bands at ~ 3300 cm^{-1}. The similarities in the IR spectra of the two compounds are obvious.

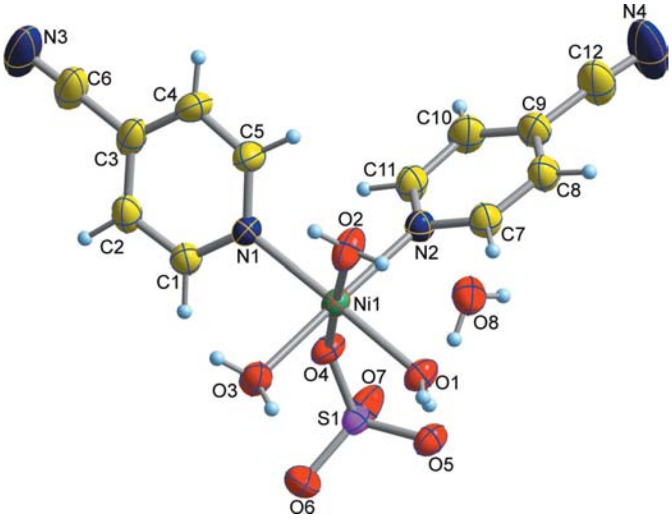

Figure 1
Molecular structure of $Ni(H_2O)_3(SO_4)(4\text{-CNpy})_2{\cdot}H_2O$ (1). Compound (2) has an analogous structure.

3.2. Crystal structure

The crystal structures of (1) and (2) have been determined by single-crystal X-ray diffraction. Crystallographic data are given in Table 1.[1] The same atom-numbering schemes for all atoms other than Ni1 and Co1 have been adopted for both compounds. The molecular structure of the nickel compound (1) is shown in Fig. 1. Selected bond distances and angles of (1) and (2) are given in Table 2. The coordination sphere of nickel in (1), and also of cobalt in (2), consists of two 4-CNpy molecules, three water molecules and one monodentate (η^1) sulfate ion as ligands. In both compounds the 4-CNpy ligands are coordinated as monodentate ligands to the Ni and Co atoms *via* the pyridyl-N atoms in a *cis* (adjacent) fashion.

The two non-equivalent Ni—N distances of 2.096 (1) and 2.153 (1) Å observed for (1) are shorter than the corresponding distances of 2.135 (1) and 2.200 (1) Å in (2). However, apart from Co1—O1 which is appreciably longer

---

[1] Supplementary data, including an *ORTEP* (Burnett & Johnson, 1996) diagram of (2), a space-filling diagram illustrating the layered crystal structure of (1) and (2), the observed and calculated X-ray powder diffraction patterns for (1) and (2), the mid-IR spectra of (1) and (2), and a crystal-packing diagram of (3), for this paper are available from the IUCr electronic archives (Reference: ZB5003). Services for accessing these data are described at the back of the journal.

Table 2
Geometric parameters (Å, °) for $M(H_2O)_3(SO_4)(4\text{-CNpy})_2\cdot H_2O$ with M = Ni (1) and M = Co (2).

Identical atom-naming schemes have been used for both structures.

	$M(H_2O)_3(SO_4)(4\text{-CNpy})_2\cdot H_2O$	
Bond parameters	M = Ni (1)	M = Co (2)
$M1$—O1	2.058 (1)	2.095 (1)
$M1$—O2	2.085 (1)	2.080 (1)
$M1$—O3	2.091 (1)	2.086 (1)
$M1$—O4	2.090 (1)	2.074 (1)
$M1$—N1	2.096 (1)	2.135 (1)
$M1$—N2	2.153 (1)	2.200 (1)
C6—N3	1.143 (3)	1.134 (3)
C12—N4	1.138 (3)	1.128 (3)
O1—$M1$—O2	88.52 (6)	88.35 (5)
O1—$M1$—O4	92.21 (5)	91.90 (5)
O2—$M1$—O4	175.37 (5)	174.38 (5)
O1—$M1$—O3	90.46 (6)	90.71 (5)
O2—$M1$—O3	93.84 (6)	93.60 (6)
O4—$M1$—O3	90.72 (5)	92.01 (5)
O1—$M1$—N1	178.50 (5)	178.88 (5)
O2—$M1$—N1	91.67 (6)	91.96 (5)
O4—$M1$—N1	87.72 (5)	87.90 (4)
O3—$M1$—N1	88.05 (6)	88.20 (5)
O1—$M1$—N2	88.34 (5)	87.83 (5)
O2—$M1$—N2	86.73 (6)	85.62 (5)
O4—$M1$—N2	88.72 (5)	88.78 (5)
O3—$M1$—N2	178.65 (5)	178.36 (5)
N1—$M1$—N2	93.15 (5)	93.26 (5)
C3—C6—N3	178.8 (3)	178.7 (3)
C9—C12—N4	176.0 (3)	176.7 (3)

	M = Ni		M = Co	
Hydrogen bonds	$d(D\cdots A)$ (Å)	$(\angle DHA)$ (°)	$d(D\cdots A)$ (Å)	$(\angle DHA)$ (°)
O1—H1$A\cdots$O6$^{\rm i}$	2.764 (2)	173 (3)	2.745 (2)	166 (2)
O1—H1$B\cdots$O5	2.729 (2)	158 (2)	2.720 (2)	161 (2)
O2—H2$A\cdots$O7$^{\rm ii}$	2.694 (2)	177 (3)	2.665 (2)	176 (3)
O2—H2$B\cdots$O8	2.892 (2)	176 (2)	2.867 (2)	177 (2)
O3—H3$A\cdots$O5$^{\rm iii}$	2.775 (2)	168 (3)	2.749 (2)	169 (3)
O3—H3$B\cdots$O8$^{\rm iv}$	2.813 (2)	178 (2)	2.785 (2)	176 (2)
O8—H8$A\cdots$O6$^{\rm v}$	2.776 (2)	157 (2)	2.758 (2)	156 (3)
O8—H8$B\cdots$O7$^{\rm vi}$	3.094 (2)	156 (2)	3.104 (2)	154 (2)
O8—H8$B\cdots$O6$^{\rm vii}$	3.107 (2)	140 (2)	3.069 (2)	143 (2)

Symmetry codes: (i) $-x, y-\frac{1}{2}, -z+\frac{3}{2}$; (ii) $x, y-1, z$; (iii) $-x, y-\frac{1}{2}, -z+\frac{3}{2}$; (iv) $x, -y+\frac{1}{2}, z+\frac{1}{2}$; (v) $-x, y-\frac{1}{2}, -z+\frac{3}{2}$; (vi) $x, -y+\frac{3}{2}, z-\frac{1}{2}$; (vii) $x, -y+\frac{3}{2}, z-\frac{1}{2}$.

than Ni1—O1, the other Co—O distances are somewhat shorter compared with the corresponding Ni—O bonds. The important point to note here is that the Co1—O4 bond of 2.074 (1) Å, which is the shortest among the six cobalt–ligand bonds in (2), is for the Co—OSO_3 bond suggesting it to be the strongest metal–ligand bond in (2). The same feature is however not observed in (1) for which the shortest nickel–ligand bond [Ni1—O1 2.058 (1) Å] is for a coordinated water molecule. While the *cis*-L—Ni—L angles range from 86.73 (6) to 93.84 (6)°, the *trans* angles are found to be 175.37 (5), 178.50 (5) and 178.65 (5)°. The observed geometrical parameters thus indicate that the coordination spheres of the metal ions deviate considerably from ideal octahedral geometry. The above observations are thus ascribable to the presence of three different types of ligand in the coordination sphere. At the same time, several intra- and intermolecular non-covalent interactions present in these otherwise simple coordination complexes (please see below) may also be responsible for these variations.

The most striking feature of the crystal structure of (1) is the presence of extensive O—H$\cdots$O hydrogen-bonding interactions involving the coordinated and uncoordinated water molecules and also the coordinated sulfato ligand (Fig. 2). The hydrogen bonds are listed in Table 2, while a crystal-packing diagram illustrating these interactions is shown in Fig. 3. It can be clearly seen that the intermolecular hydrogen bonds direct the complex molecules, $[M(H_2O)_3(SO_4)(4\text{-CNpy})_2]$, and the H_2O molecules present as a solvent of crystallization in (1) and (2) to organize into two-molecule thick layers formed because of the partitioning of the inorganic and organic

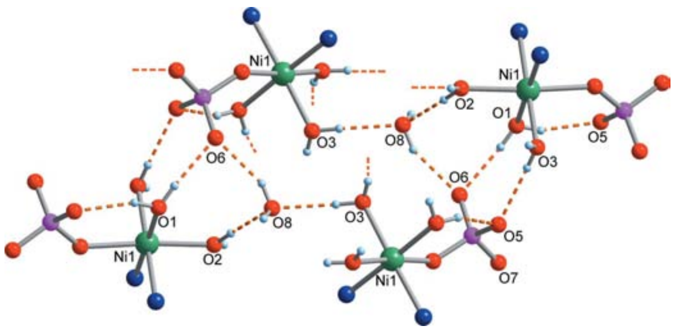

Figure 2
Hydrogen bonds in the crystal structure of (1). Only the coordinated N atoms of the 4-CNpy ligands are shown for clarity. Similar diagrams may also be drawn for (2). This figure is in colour in the electronic version of this paper.

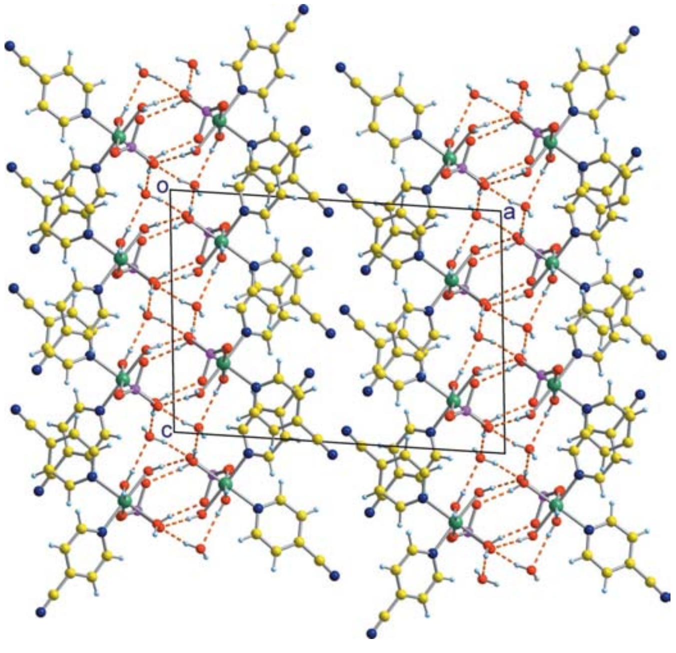

Figure 3
Crystal-packing diagram of $Ni(H_2O)_3(SO_4)(4\text{-CNpy})_2\cdot H_2O$ (1), showing its layered structure as viewed down the crystallographic b axis. A nearly identical diagram can also be generated for (2).

moieties as guided by non-covalent forces. These bilayers run along the crystallographic *bc* plane.

3.2.1. Graph-set analysis of hydrogen bonds. The crystal structure of (1) [and also (2)] is characterized by as many as nine distinct O—H···O hydrogen bonds in the solid state (Table 2). The presence of these hydrogen bonds creates intricate patterns within the layers that can be analyzed by graph-set theory (Bernstein *et al.*, 1995). It is first noted that the coordinated as well as uncoordinated water molecules along with the sulfato ligands are self-assembled to form helical supramolecular chains. Two such chains of descriptors $C_3^3(8)$ and $C_3^3(6)$ run approximately along the crystallographic *c* axis. The superscripts and subscripts in the above graph-set notations are, respectively, the number of hydrogen-bond acceptors and hydrogen-bond donors. Along the direction of these chains there is a periodic repetition of a ten-membered ring and an eight-membered ring. The former ring is describable as an $R_5^3(10)$ graph set, whereas the latter is $R_2^2(8)$. Additionally, an intramolecular hydrogen-bonded ring is also present in the crystal lattice. This ring of the type 'Ni—$O_{sulfate}$—S—$O_{sulfate}$—(OH_2)' is designated as *S*(6). The patterns as described above are depicted in Fig. 4.

3.2.2. *π*–*π* interactions between nitrile groups. As can be seen from Fig. 3, the interlayer space is occupied by the nitrile groups from the 4-CNpy ($-NC_5H_4$-*p*-CN) ligands. The —C≡N groups protruding out of one of the two 4-CNpy moieties from each complex are aligned in an antiparallel manner, as illustrated in Fig. 5. The close proximity of the nitrile groups may be an outcome of *π*–*π* interactions involving the —C≡N groups. Such interactions of moderate strength appear to be possible because of the perfect antiparallel alignment of the triple bonds present in the nitrile groups from two adjacent layers. The closest centroid-to-centroid distances between the *π* systems of two —C≡N fragments of the 4-CNpy ligands in (1) and (2) are 3.736 (4) and 3.711 (5) Å, respectively (Fig. 5). It has been recently reported for Zn^{II} and Sn^{IV} complexes of dipyrido[*f*,*h*]quinoxaline-6,7-dicarbonitrile that dipole–dipole interactions between —C≡N groups is one of several types of non-covalent contacts involved in the intermolecular organization of the complexes (Kozlov & Goldberg, 2008). The most notable feature of our structures is that instead of the (C)N···*π*(C≡N) dipolar interaction, *π*–*π* proximity between —C≡N and N≡C— have guided the intermolecular organization into the observed bilayer structure of the title compounds. In hindsight, we also note with interest here that similar interactions between nitrile groups also characterize the crystal structure of $Cu_2(\mu\text{-}O_2CCH_3)_2(4\text{-CNpy})_2$ (3), a dimeric copper(II) compound which has been previously reported (Das & Barman, 2001). In this crystal structure the two closest nitrile groups show a centroid-to-centroid separation of 3.473 (9) Å. See supplementary material.

Among the two nitrile groups of the mutually *cis* 4-CNpy ligands in each complex, only one is involved in a possible *π*–*π* interaction. It is interesting to note that in both compounds there is very little, if any, influence of the assumed interaction on the C≡N triple bond strength, as indicated by the nearly equal C≡N distances for the nitrile groups in each compound. It may also be pointed out that any such effect is also not emphatically shown in the *ν*(C≡N) vibrations observed for the compounds (see above). In view of such contraindicative results we took recourse to theoretical investigations to gain an understanding of the apparent *π*–*π* interaction between antiparallel nitrile (—C≡N) groups in the crystal structure of (1). Both Hartree–Fock (HF) and DFT calculations have been performed employing *GAUSSIAN*03W for (1) using the

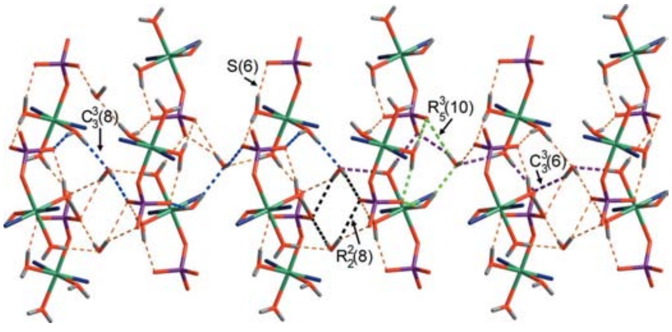

Figure 4
The hydrogen-bonded patterns designated by graph-set descriptors found in the crystal structure of (1) and (2). For clarity, the 4-CNpy ligands have been denoted by only the pyridyl-N atoms.

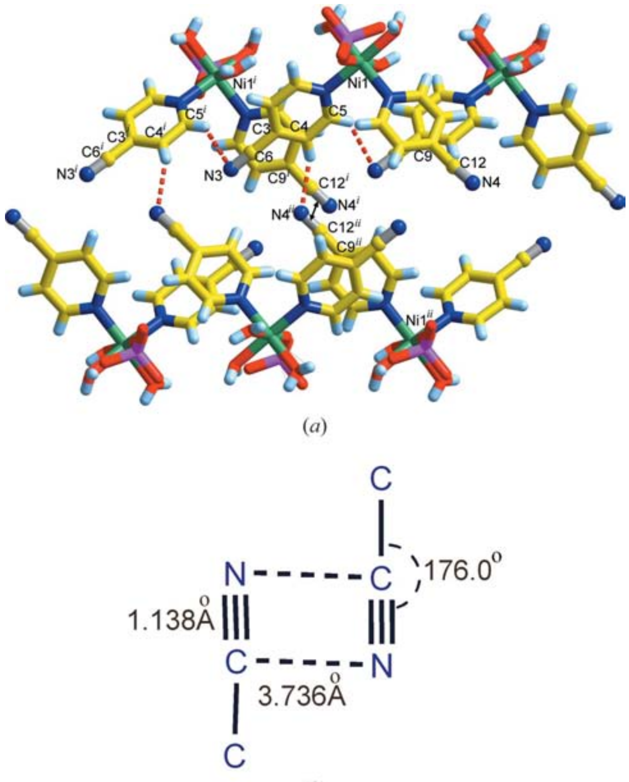

(*a*)

(*b*)

Figure 5
(*a*) *π*–*π* interactions (double-headed arrow) observed between the antiparallel —C≡N fragments from two adjacent layers. The intermolecular C—H···N interactions observed in the crystal structure of (1) are shown as dotted lines. (*b*) Schematic representation of the antiparallel nitrile groups in the crystal structure of (1).

Table 3
C—H···N bridges for (1) and (2).

D—H···A	d(H···A) (Å)	d(D···A) (Å)	∠D—H···A (°)
(1)			
C5^{i}—H···N3	2.699 (2)	3.412 (3)	134.09 (11)
C4—H···N4^{ii}	2.526 (2)	3.342 (3)	146.85 (12)
(2)			
C5^{i}—H5···N3	2.669 (3)	3.391 (3)	134.99 (11)
C4—H4···N4^{ii}	2.503 (2)	3.323 (3)	147.31 (11)

Symmetry codes: (i) $x, \frac{1}{2} - y, \frac{1}{2} + z$; (ii) $1 - x, \frac{1}{2} + y, \frac{3}{2} - z$.

atomic coordinates obtained from single-crystal X-ray diffraction data. For this purpose we chose a system composed of two molecular units of (1), in which the nitrile groups are closest to one another (Fig. 6). The interaction energy has been calculated using the equation $\Delta E = E_{AB} - (E_A + E_B)$, where ΔE denotes the interaction energy, and E_{AB}, E_A and E_B denote the stabilization energies of both molecules A and B together, molecule A and molecule B. Both levels of theoretical treatment gave consistent results showing stabilization for the A and B arrangement compared with the sum of individual A and B molecules. The stabilization energies are found to be −87.34 and −128.91 kJ mol^{-1} on the basis of HF and DFT calculations. Notwithstanding the numerical difference between the two values of energy, these negative interaction energies certainly indicate the existence of moderately strong π–π interactions between the antiparallel nitrile moieties.

While recognizing the above π–π interaction as a stabilizing force it is also important to keep in mind that in the antiparallel alignment of the nitrile groups the lone pair of electrons on N will come close to the relatively electron-poor C. Thus, an electrostatic attraction also accompanies any possible interaction between the C≡N π systems. A combination of two such forces was also considered (Janiak, 2006) to be favourable in assumed π–π interactions involving aromatic rings. However, the correct estimation of these and other forms of non-covalent interaction energies by various methods of calculation may be quite difficult (Tateno & Hagiwara, 2009). The interaction or stabilization energy obtained for (1) should thus be viewed in this light. Phenomenologically, however, it is convenient to point out that the C—C≡N angles ∠C9—C12—N4 are slightly smaller than ∠C3—C6—N3 in (1) and (2). For (1) these values are 176.0 (2) and 178.8 (2)°, while for (2) the values are 176.7 (2) and 178.8 (2)° (see Fig. 5*b*). This increased bending of the C—C≡N angle in each structure probably constitutes a measure of intermolecular interactions involving the nitrile functional groups attached to aromatic rings. The present observation points to the identification of a new supramolecular synthon which may prove useful in the design of novel supramolecular solids (Desiraju, 2001).

3.2.3. C—H···N contacts. In addition to O—H···O hydrogen bonds present in the crystal structure of (1) and (2), another important factor is the weak intermolecular C—H···N hydrogen bond. Fig. 5 illustrates the intra- and interlayer C—H···N hydrogen bonds. The nitrile groups of 4-CNpy ligands are acceptors for the C—H donors from 4-CNpy ligands of nearby complex molecules. These hydrogen bridges have C···N distances of 3.342 (3) and 3.412 (3) Å for (1) and 3.323 (3) and 3.391 (3) Å for (2), all consistent with the similar weak hydrogen bonds reported earlier (Stephenson & Hardie, 2006; Yu, 2007; Kozlov & Goldberg, 2008). Details of these non-covalent interactions are listed in Table 3.

The bond parameters for the C—H···N hydrogen bridges indicate the inherent weakness of such interactions. Nevertheless, the existence of many such interactions is likely to enhance the stability of the solid-state assemblies resulting exclusively from supramolecular forces.

3.2.4. Isostructurality of (1) and (2). It has already been amply clear from the above discussion that from a crystallographic angle compounds (1) and (2) are quite analogous because these two species differ only on the basis of the metal ions present in them. Such structurally related compounds may be said to belong to the same structure type. Confirming their close structural similarity, the X-ray powder diffraction patterns recorded for the compounds are also found to be

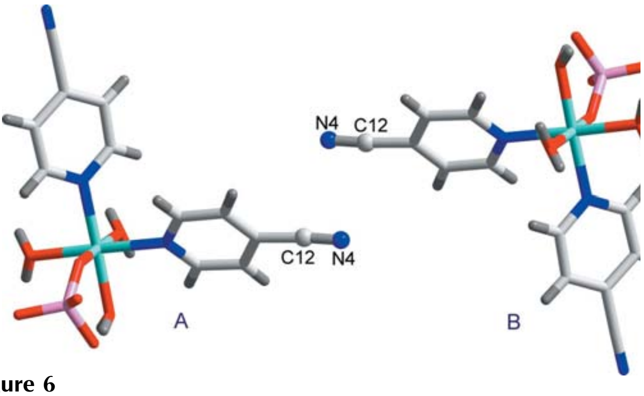

Figure 6
Two neighbouring molecular units of (1) showing an antiparallel alignment of C≡N groups involved in a π–π interaction.

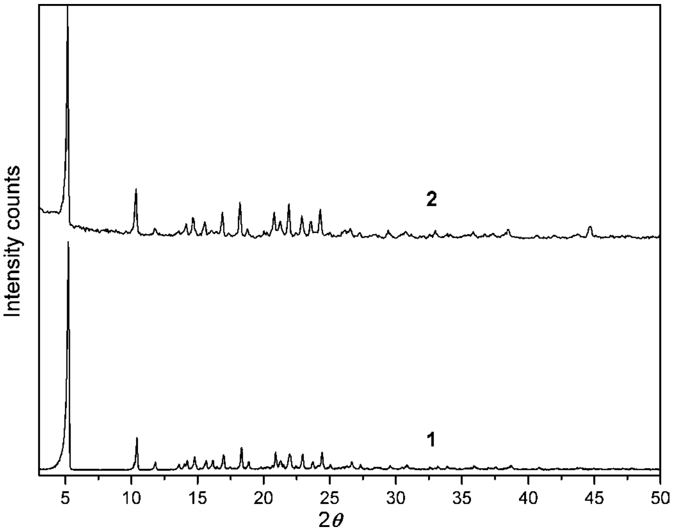

Figure 7
The X-ray powder diffraction patterns recorded for (1) and (2).

analogous (Fig. 7). Furthermore, the experimental and calculated X-ray powder diffraction patterns for both compounds match very well to suggest that the crystals examined by single-crystal X-ray diffraction in the two cases are truly representative of the bulk samples prepared by us.

The isostructurality of the two crystals has also been evaluated according to the approach of Fábián & Kálmán (1999) in which two structures may be compared by a parameter called the unit-cell similarity index given by $\Pi = [(a+b+c)/(a'+b'+c')] - 1$, where $(a+b+c > a'+b'+c')$. Here a, b, c and a', b', c' are the orthogonalized lattice parameters of the structures being examined. If the structural similarity is very high, the Π value is expected to be practically equal to zero (Fábián & Kálmán, 1999). In our case the value is estimated to be 0.0046, which corroborates the close structural similarity obtained from crystal structure analyses. In view of the fact that it is possible to prepare analogous metal-organic compounds involving bivalent metal ions of the first transition series (Das *et al.*, 2006), the preparation of more compounds having the isostructural relationship with (1) and (2) appears to be possible. Indeed, it will be worth examining the possibilities of obtaining molecular alloys (Dechambenoit *et al.*, 2009) by making use of such isostructural metal complexes.

4. Conclusions

Two analogous crystalline species of the chemical formula $M(H_2O)_3(SO_4)(4\text{-CNpy})_2\cdot H_2O$ (M = Ni and Co) have been synthesized and characterized by X-ray diffraction. The structure of the coordination solids is stabilized by several non-covalent interactions including an interesting type of π–π interaction involving nitrile groups present in 4-CNpy ligands. The π–π interactions involving antiparallel nitrile groups from two different hydrogen-bonded bilayers are given credence by Hartree–Fock as well as DFT calculations using *GAUSSIAN*03W. Commensurate with the observed similarity of the supramolecular structures of (1) and (2), the X-ray powder diffraction patterns shown by the two compounds are also analogous. In addition, as suggested by the Π index of Fábián & Kálmán (1999), the two crystal structures under investigation are isostructural. Based on the π–π interactions involving nitrile groups present in the 4-cyanopyridine ligands and also the isostructurality of the complexes, the synthesis of other supramolecular compounds including molecular alloys formed from them appears to be possible.

Financial support from Department of Science & Technology (FIST) and University Grants Commission (DSA), India, is gratefully acknowledged. The authors thank Professor M. G. Kanatzidis, Michigan State University (now at Northwestern University), USA, and the Department of Chemistry, Indian Institute of Technology, Guwahati, for help in obtaining single-crystal X-ray data on (1) and (2), respectively.

References

Barman, R. K. & Das, B. K. (2002). *CrystEngComm*, pp. 80–83.

Beatty, A. M., Schneider, C. M., Simpson, A. E. & Zaher, J. L. (2002). *CrystEngComm*, **4**, 282–287.

Bernstein, J., Davis, R. E., Shimoni, L. & Chang, N.-L. (1995). *Angew. Chem. Int. Ed. Engl.* **34**, 1555–1573.

Bhattacharyya, M. K., Bora, S. J. & Das, B. K. (2008). *J. Chem. Cryst.* **38**, 195–203.

Biradha, K., Dennis, D., MacKinnon, V. A., Sharma, C. V. K. & Zaworotko, M. J. (1998). *J. Am. Chem. Soc.* **120**, 11894–11903.

Bora, S. J. & Das, B. K. (2009). In preparation.

Brandenburg, K. (2008). *DIAMOND*, Version 3.1f. Crystal Impact, GbR, Bonn, Germany.

Bruker AXS Inc. (2004*a*). *SMART*. Bruker AXS Inc., Madison, Wisconsin, USA.

Bruker AXS Inc. (2004*b*). *SAINT*. Bruker AXS Inc., Madison, Wisconsin, USA.

Burnett, M. N. & Johnson, C. K. (1996). *ORTEP*III, Report No. ORNL-6895. Oak Ridge National Laboratory, Oak Ridge, Tennessee, USA.

Chakrabarty, R., Bora, S. J. & Das, B. K. (2007). *Inorg. Chem.* **46**, 9450–9462.

Cotton, F. A. & Wilkinson, G. (1988). *Advanced Inorganic Chemistry*, p. 488. New York: John Wiley and Sons.

Das, B. K. & Barman, R. K. (2001). *Acta Cryst.* C**57**, 1025–1026.

Das, B. K., Bora, S. J., Chakrabortty, M., Kalita, L., Chakrabarty, R. & Barman, R. K. (2006). *J. Chem. Sci.* **118**, 487–494.

Dechambenoit, P., Ferlay, S., Kyritsakas, N. & Hosseini, M. W. (2009). *Chem. Commun.* pp. 2514–2516.

Desiraju, G. R. (2001). *Nature*, **412**, 397–400.

Fábián, L. & Kálmán, A. (1999). *Acta Cryst.* B**55**, 1099–1108.

Farrugia, L. J. (1999). *J. Appl. Cryst.* **32**, 837–838.

Frisch, M. J. *et al.* (2004). *GAUSSIAN*03, Version 6.1. Gaussian, Inc., Wallingford CT, USA.

Holman, K. T., Pivovar, A. M., Swift, J. A. & Ward, M. D. (2001). *Acc. Chem. Res.* **34**, 107–108.

Janiak, C. (2006). *J. Chem. Soc. Dalton Trans.* pp. 3885–3896.

Kozlov, L. & Goldberg, I. (2008). *Acta Cryst.* C**64**, m123–m126.

Kraus, W. & Nolze, G. (2000). *PowderCell for Windows*, Version 2.4. Berlin: Federal Institute for Materials Research and Testing.

Macrae, C. F., Edgington, P. R., McCabe, P., Pidcock, E., Shields, G. P., Taylor, R., Towler, M. & van de Streek, J. (2006). *J. Appl. Cryst.* **39**, 453–457.

Nakamoto, K. (1978). *Infrared and Raman Spectra of Inorganic and Coordination Compounds*, p. 239. New York: John Wiley and Sons.

Originlab (2007). *Origin*® 8. The Data Analysis and Graphing Workspace. Originlab Corporation, Northampton, MA, USA.

Raghavaiah, P., Supriya, S. & Das, S. K. (2005). *CrystEngComm*, **7**, 167–170.

Sheldrick, G. M. (2008). *Acta Cryst.* A**64**, 112–122.

Spek, A. L. (1990). *Acta Cryst.* A**46**, C34.

Stephenson, M. D. & Hardie, M. J. (2006). *Cryst. Growth Des.* **6**, 423–432.

Tateno, M. & Hagiwara, Y. (2009). *J. Phys. Condens. Matter*, **21**, 1–7.

Yu, M. (2007). *Acta Cryst.* E**63**, o2863.